ORIGINAL ARTICLE

Coating sponge with a hydrophobic porous coordination polymer containing a low-energy CF$_3$-decorated surface for continuous pumping recovery of an oil spill from water

Zhuo-Rui Jiang[1,3], Jin Ge[1,3], Yu-Xiao Zhou[1,3], Zhiyong U Wang[2], Dongxiao Chen[1], Shu-Hong Yu[1] and Hai-Long Jiang[1]

For the remediation of oil spills and organic solvent leakage into water, it is desirable to develop not only advanced sorbents with a high adsorption capability but also labor- and time-saving apparatuses that can work continuously without human intervention. In this work, we synthesized a novel and highly stable porous coordination polymer (PCP, also called metal-organic framework), University of Science and Technology of China-6 (USTC-6), with a corrugated -CF$_3$ surface that features high hydrophobicity. The uniform growth of USTC-6 throughout a graphene oxide (GO)-modified sponge was achieved and yielded a macroscopic USTC-6@GO@sponge sorbent, which repels water and exhibits a superior adsorption capacity for diverse oils and organic solvents. Remarkably, the sorbent can be further assembled with tubes and a self-priming pump to build a model apparatus that affords consecutive and efficient oil recovery from water. The easy and fast recovery of oils/organic solvents from water based on such an apparatus indicates that it has great potential for future water purification and treatment.

INTRODUCTION

The explosion of the BP Deepwater Horizon oil rig in the Gulf of Mexico in 2010 and the grounding of a container ship in New Zealand in 2011 caused colossal economic damage and environmental disasters. Oil spills are difficult to clean up and thus result in severe long-lasting damage to the marine ecosystem.[1] To develop effective technologies for oil spill remediation, in addition to dispersants and solidifiers, porous sorbents are very promising.[2] The ideal porous sorbents for oil cleanup should be hydrophobic and oleophilic to guarantee that they selectively adsorb/absorb oily target compounds but not water. The generation of a biomimetic rough surface on nano-to-micrometer scaled porous materials has been demonstrated to be an effective strategy to enhance their hydrophobicity.[3,4] Thus far, various porous sorbents, such as resins, gels, carbon-based sponges/solids and diverse polymeric materials, have been explored.[5–8] Previous studies have excessively focused on the oil sorption capacity, and the spilled oil has been recovered mainly via distillation and squeezing,[9–12] which are time-consuming, tedious and energy-demanding and are thus seriously restricted in their practical application.

To achieve regulation of the rough hydrophobic surface of oil sorbents at the molecular level, porous coordination polymers (PCPs), also called metal-organic frameworks,[13–15] may be one of the most ideal porous materials. Significant advantages of PCPs over traditional porous materials include their crystalline nature, structural diversity and high tunability and tailorability, which make them suitable for a variety of applications, such as gas adsorption and separation, catalysis, sensing and proton conductivity.[16–32] Oil spill cleanup and recovery from water is one area in which PCPs may have very promising application potential. However, to our knowledge, it is very rare for PCPs to be used for such an application because of two major challenges.[33] First, the separation of oil from water requires PCPs to be water stable. Although some water-stable PCPs have been developed,[34–40] most PCPs are actually sensitive toward moisture. Second, PCPs need to have hydrophobic surfaces to prevent the entry of water molecules into the pores. Of the various strategies that have evolved to produce water-stable hydrophobic PCPs, the incorporation of fluorine into PCPs is particularly effective.[41–47]

Therefore, we are interested in developing fluorous PCPs for oil spill cleanup and recovery as corrugated PCP surfaces with -CF$_3$

[1]Hefei National Laboratory for Physical Sciences at the Microscale, CAS Key Laboratory of Soft Matter Chemistry, Collaborative Innovation Center of Suzhou Nano Science and Technology, Department of Chemistry, University of Science and Technology of China, Hefei, PR China and [2]Department of Chemistry and Physics, Troy University, AL, USA
[3]These authors contributed equally to this work.
Correspondence: Professor S-H Yu or Professor H-L Jiang, Department of Chemistry, University of Science and Technology of China (USTC), No. 96 Jinzhai Road, Hefei, Anhui 230026, PR China.
E-mail: (shyu@ustc.edu.cn or jianglab@ustc.edu.cn)

alignment may render it very hydrophobic.[33,46–49] We thus envision that a ligand with -CF$_3$ groups will give PCPs a high fluorine content and may boost their hydrophobicity. The compound 4,4'-(hexafluoroisopropylidene)diphthalate (H$_4$L) was chosen as the ligand, and it reacts with CuCl$_2$·2H$_2$O under solvothermal conditions to yield blue brick-shaped crystals with the formula [Cu$_3$(H$_2$L)$_4$(H$_2$O)$_2$][Cu(H$_2$O)$_6$]·(H$_2$O)$_2$ (University of Science and Technology of China-6 (USTC-6)), based on single crystal X-ray diffraction, thermogravimetric and elemental analyses (Supplementary Figures S2 and S4–S6).

EXPERIMENTAL PROCEDURES

Preparation of USTC-6 (single crystals)
A mixture of CuCl$_2$·2H$_2$O (12 mg), 4,4'-(hexafluoroisopropylidene)diphthalic anhydride (10 mg) and deionized water (2 ml) was sealed in a 5-ml vial and heated at 358 K for 24 h. After cooling down to room temperature, the resulting blue crystals were washed with water three times to give USTC-6 (7.2 mg, 57.9% based on ligand). The X-ray photoelectron spectroscopy measurements confirmed the presence of Cu, C, O and F elements in the crystals (Supplementary Figure S4). Infrared Analysis (KBr, cm^{-1}): 3449 (b), 1705 (vs), 1630 (s), 1572 (s), 1508 (m), 1424 (vs), 1313 (s), 1268 (s), 1211 (s), 1185 (s), 1145 (w), 1082 (m), 989 (m), 957 (m), 850 (m), 793 (m), 780 (m), 721 (w), 519 (m), 455 (w). Elemental analysis calcd (%) for USTC-6: C 38.88, H 2.23; found: C 37.52, H 2.37.

Preparation of USTC-6 (powder)
A mixture of CuCl$_2$·2H$_2$O (12 mg), 4,4'-(hexafluoroisopropylidene)diphthalic anhydride (10 mg), deionized water (0.5 ml) and *N'N*-dimethylformamide (DMF) (1.5 ml) was sealed in a 5-ml vial and heated at 358 K for 24 h. After cooling down to room temperature, the resulting blue powder was washed with water three times. Upon removal of the solvent and drying in vacuum at 25 °C, USTC-6 (powder, 8.3 mg, 66.7% based on the ligand) was obtained.

Preparation of nanosized USTC-6
A mixture of CuCl$_2$·2H$_2$O (12 mg), 4,4'-(hexafluoroisopropylidene)diphthalic anhydride (10 mg), deionized water (1.5 ml), DMF (0.5 ml) and NH$_3$·H$_2$O (30 µl) was sealed in a 5-ml vial and heated at 358 K for 24 h. After cooling down to room temperature, the resulting blue slurry was filtered and washed with water. Upon drying in vacuum at 25 °C, nanosized USTC-6 was obtained as a blue powder (9.9 mg, 79.6% based on the ligand).

Preparation of GO@sponge
A commercially available macroporous sponge was cleaned by water and ethanol several times, followed by drying at 100 °C for 24 h and cutting into small cubes (approximately 2 × 2 × 2 cm^3). All of the sponges were dipped into graphene oxide (GO) (approximately 2.6 mg ml^{-1}) prepared according to a reported method,[50] taken out and centrifuged at 3000 r.p.m. for 2 min to remove the excessive uncoated GO, and finally dried in an oven at 100 °C for 24 h.

Preparation of USTC-6@GO@sponge with nanosized USTC-6
A mixture of CuCl$_2$·2H$_2$O (450 mg), 4,4'-(hexafluoroisopropylidene)diphthalic anhydride (300 mg), deionized water (37.5 ml), DMF (12.5 ml) and NH$_3$·H$_2$O (1 ml) was placed in a 100-ml Teflon-capped autoclave and sonicated to make a homogeneous solution. The pre-prepared GO@sponge was put into the solution, and the autoclave was then sealed and heated at 358 K for 24 h. After cooling down to room temperature and dried in vacuum at 25 °C, the resulting light-blue USTC-6@GO@sponge with nanosized USTC-6 was obtained.

Preparation of USTC-6@GO@sponge
A mixture of CuCl$_2$·2H$_2$O (450 mg), 4,4'-(hexafluoroisopropylidene)diphthalic anhydride (300 mg), deionized water (10 ml) and DMF (30 ml) was placed in a 100-ml Teflon-capped autoclave and sonicated to make a homogeneous solution. The pre-prepared GO@sponge was put into the solution, jand the autoclave was then sealed and heated at 358 K for 24 h. After cooling down to room temperature and being dried in a vacuum at 25 °C, the resulting blue USTC-6@GO@sponge was obtained with a USTC-6 loading of approximately 70%.

Oil/organic solvent removal tests
Different types of organic solvents and oils with different densities, including diesel oil, gasoline, soybean oil, light petroleum, *n*-hexane, bromobenzene, DMF, tetrahydrofuran, acetone, CCl$_4$ and methylbenzene, were used in this study. Weight gain, wt%, was obtained by measuring the mass of the USTC-6@GO@sponge sorbent, and then the total mass after oil/solvent absorption. The sorbent was left submerged in the solvents or oils for a few seconds before weighing. Weight measurements were conducted rapidly to avoid evaporation of adsorbed solvents or oils.

Fabrication of the oil collection apparatus
One end of a Teflon tube was inserted into the USTC-6@GO@sponge sorbent, and the other end was connected to the inlet of the self-priming pump that was driven by a 4.5-V power supply unless otherwise mentioned. Then, the outlet of the self-priming pump was connected to another Teflon tube that was introduced to the collection vessel.

Single-crystal X-ray crystallography
Crystal data were collected on an Oxford Diffraction Gemini S Ultra CCD diffractometer at room temperature with Cu-Kα radiation (λ = 1.54 Å). The structure was solved by direct methods using the SHELXS program of the SHELXTL package and refined by full-matrix least-squares methods with SHELXL.[51] Metal atoms were located from the E-maps and other non-hydrogen atoms were located in successive difference Fourier syntheses, all of which, except for O2w, were refined with anisotropic thermal parameters on F^2. The hydrogen atoms of the ligands were theoretically generated onto the specific atoms and isotropically refined with fixed thermal factors. The Cu(3) atom located at a general position has only a 25% possibility. The hydrogen atoms of the water molecules were not defined. The disordered O2w, O2w', O3w, O4w' and O6w atoms were all split into two positions. All of the crystallographic and structure refinement data for the compound are summarized in Supplementary Table S1. (Related structure information can be also found in the Supplementary data.)

Crystal data for USTC-6
C$_{76}$H$_{52}$Cu$_4$F$_{24}$O$_{42}$; refined formula weight, M_r = 2347.37 g mol^{-1}; monoclinic, space group C2/m, a = 10.820(2) Å, b = 37.260(7) Å, c = 11.550(2) Å, β = 100.17 (3)°, V = 4583.3(14) Å^3; Z = 2; calculated cell density, D_c = 1.686 g cm^{-3}; reflections collected/independent: 10 121/4317; R_{int} = 0.0294; final R_1 = 0.0705 ($I > \sigma$ (I)), wR_2 = 0.0720 (all data), goodness-of-fit (GOOF) = 1.148. Supplementary crystallographic data for this study can be obtained free of charge from the Cambridge Crystallographic Data Centre (CCDC) via www.ccdc.cam.ac.uk/data_request/cif: CCDC 1414128.

RESULTS AND DISCUSSION
USTC-6 crystallizes in the C2/m space group, and its asymmetric unit involves three crystallographically unique Cu(II) ions occupying sites in a mirror plane and one independent ligand, as well as four coordinated water and two isolated water molecules. Two Cu(1) atoms are coordinated by four carboxylates from four ligands to form a Cu$_2$(COO)$_4$ paddle-wheel cluster, and the axial position of each Cu (1) is occupied by one oxygen to give a square pyramid (Figure 1a). The Cu(2) atom lying in a position with a twofold symmetry is coordinated by four oxygens from four ligands, whereas Cu(3) is surrounded by five terminal water molecules. Among the eight oxygens from the four carboxylates in the ligand, only two oxygens from one carboxylate coordinate to the Cu(1)$_2$ cluster in a chelating mode, and another oxygen bridges with the Cu(2) atom, whereas all other oxygens remain uncoordinated (Figure 1a). Such a connection

fashion for Cu(1), Cu(2) and the ligand leads to novel 1D nanoribbons with widths of approximately 2.0 and 1.8 nm in the *a* and *b* directions, respectively (Figure 1b and c). The interconnection of 1D nanoribbons, together with the isolated water molecules and the uncoordinated $Cu(3)O_5$ units located inside the channels along the *c*-axis, via a complicated system with multiple hydrogen bonds gives a
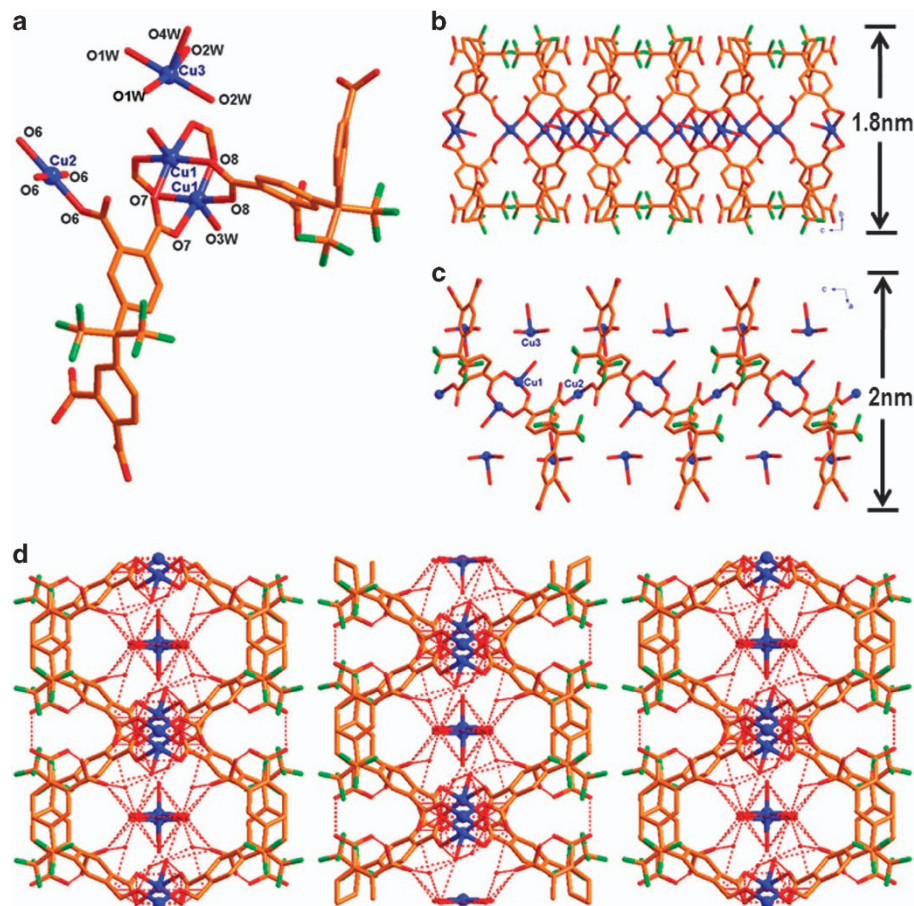

Figure 1 (a) The structure fragment of USTC-6 showing the coordination environments of Cu(II) ions and the ligand. A view of the nanoribbon with retained $Cu(3)O_5$ units along the (b) *a* axis and (c) *b* axis. The hydrogen bonding and isolated water molecules are omitted for clarity. (d) A view of the layered structure of USTC-6 along the *c* axis. The hydrogen bonds are indicated by dotted lines. The Cu, C, O and F atoms are drawn in blue, orange, red and green, respectively. All of the hydrogen atoms were omitted, and only one orientation of the disordered O2w remains for clarity.
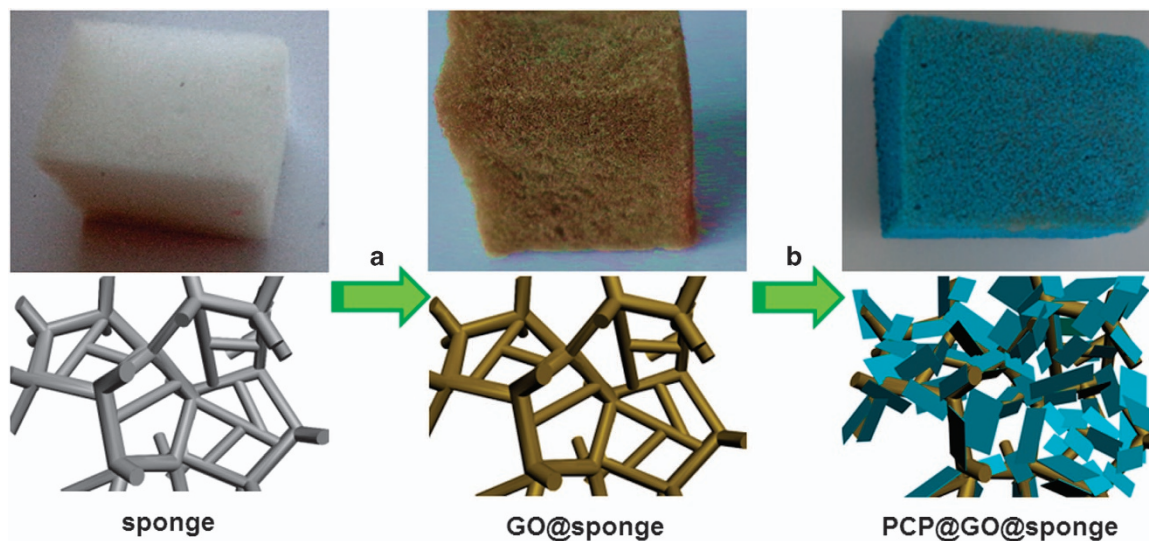
Scheme 1 Schematic illustration of the synthetic route for USTC-6@GO@sponge and the photographs showing the well-retained morphology, although there is a significant color change for the macroscopic sponge, GO@sponge and USTC-6@GO@sponge: (a) GO coating and (b) *in situ* PCP growth.

2D layer in the *ac* plane with wave-like surfaces, where -CF$_3$ groups are mounted in between the layers (Figure 1d and Supplementary Figure S1). Such a particularly roughened surface is also called 'low-energy surface'[4] with -CF$_3$ groups that repel water molecules, resulting in the high hydrophobicity of USTC-6. The interlayer distance is 18.6 Å with the -CF$_3$ groups hanging on the layer edges. The closest F…F distance between adjacent layers is only 4.5 Å, generating a narrow hydrophobic interlayer space that fully prevents the entry of water molecules (Figure 1d).

The powder X-ray diffraction data for the crystals reveal a high phase purity exhibiting a preferential orientation along the [060] direction (Supplementary Figure S2). The most exposed [060] surface possesses not only -CF$_3$ groups but also nanoscaled corrugation, generating high hydrophobicity for USTC-6, which is proved by a water contact angle of up to 132 °C for its crystals (Supplementary Figure S7). By comparison, different organic hydrocarbons can be rapidly adsorbed by USTC-6, suggesting its strong oleophilic properties. To date, some PCPs have been reported to be hydrophobic upon a postsynthetic modification with alkyl or fluoroalkyl groups;[41,42,46,47] however, very few pristine PCPs have been reported to display such a high hydrophobicity.[33,43,45] To our knowledge, USTC-6 is a very rare

highly hydrophobic PCP bearing a low-energy rough surface decorated with -CF$_3$ groups.

It is generally thought that the Cu-O (carboxylate) coordination bond in PCPs is vulnerable to hydrolysis. Strikingly, USTC-6 retains its framework in water for over 1 month and it is even stable in solutions with pH ranging from 2 to 10 for up to 7 days (Supplementary Figure S3). We assume that the hydrophobic -CF$_3$ groups are responsible for the superior stability of USTC-6.

By taking advantage of its great stability, hydrophobicity and oleophilicity, USTC-6 may be an ideal candidate for the separation of oil/organic solvents from water. To facilitate a large scale separation, however, it is desirable to integrate the PCP into a macroscopic host matrix to achieve the facile diffusion of oil and organic solvents. We chose to work with sponge, a commercially available cheap macro-porous material. We envision that the branches of sponge will be first wrapped with GO to provide a surface rich in hydroxy, carboxylic and epoxy groups, which would subsequently coordinate with metal ions and allow for the *in situ*, uniform formation and attachment of USTC-6 to yield a USTC-6@GO@sponge composite (Scheme 1).

Coating a sponge with GO was conveniently conducted by dipping the sponge into GO solution, centrifugation and drying. The scanning electron microscopy (SEM) image of GO@sponge is shown in
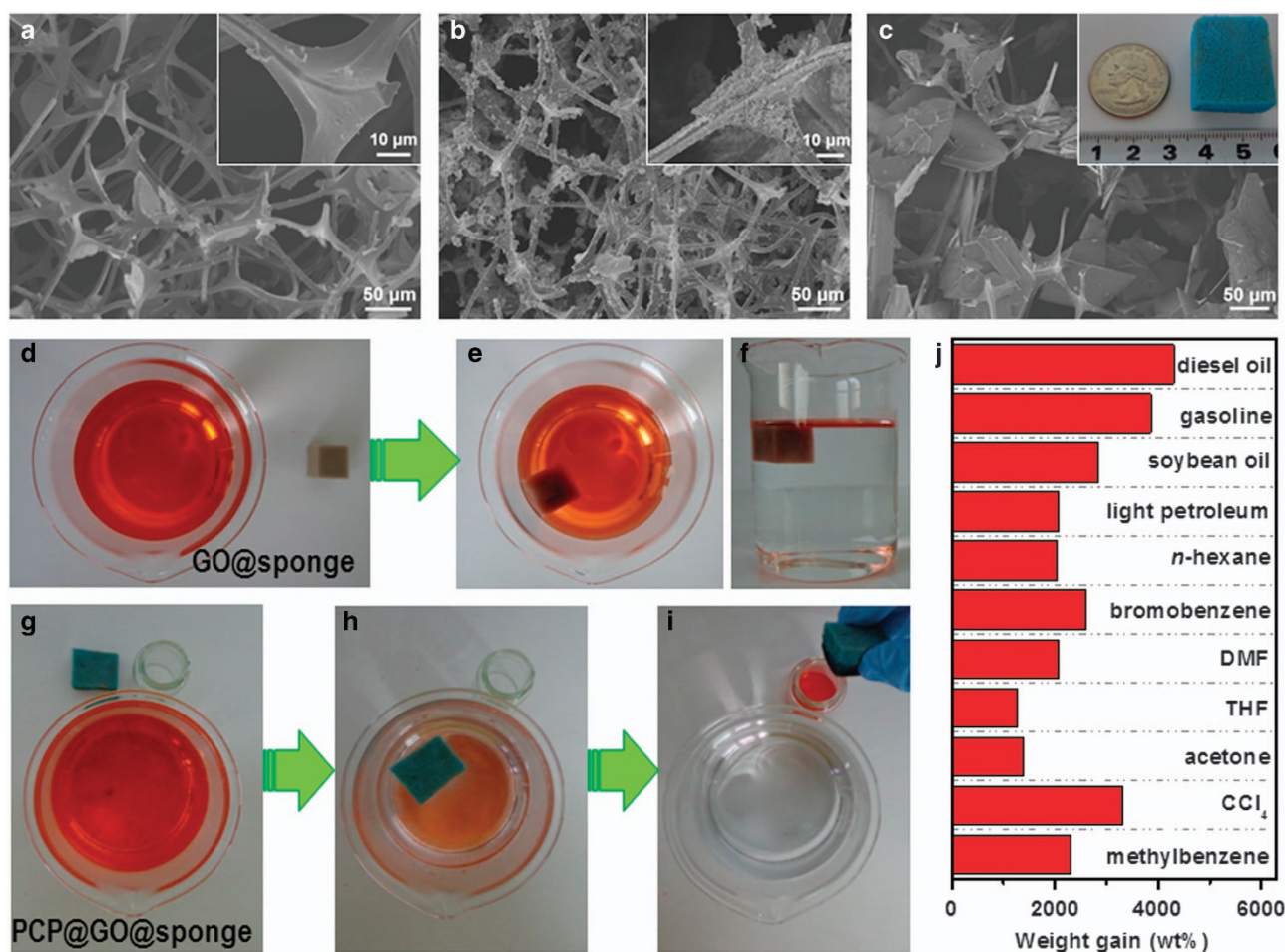

Figure 2 Scanning electron microscopy images for (**a**) GO@sponge and USTC-6@GO@sponge with (**b**) small and (**c**) large USTC-6 particles. The insets in (**a**) and (**b**) are enlarged details for the respective microstructures, whereas the inset in (**c**) shows a photograph of the macroscopic USTC-6@GO@sponge. (**d–f**) Photographs showing the non-selective adsorption behavior of GO@sponge for gasoline (dyed red) and water. (**e**) Top and (**f**) side view for GO@sponge and the liquid mixture. (**g–i**) Photographs showing gasoline uptake by USTC-6@GO@sponge and subsequent squeezing to recover the gasoline. (**j**) The adsorption efficiency of USTC-6@GO@sponge for diverse oils and organic solvents.

Figure 2a. Because both sponge and GO are amphiphilic, the GO@sponge has poor selectivity for water, oil or organic solvents (Supplementary Figure S8a–c). In a gasoline/water mixture, GO@sponge adsorbed gasoline and water together and then sank under the liquid surface (Figures 2d–f). We then attempted to grow USTC-6 *in situ* onto GO@sponge by heating GO@sponge. To our delight, this key step worked well, and we were able to achieve controlled sizes of USTC-6 on GO@sponge by simply regulating synthetic parameters (Figures 2b and c). The presence of GO on the sponge is beneficial for stabilizing and growing more PCP particles inside the pore walls of the sponge. No or negligible GO leaching occurred with GO@sponge during the growth of USTC-6 based on the Raman spectra (Supplementary Figure S9), indicating the stability of GO coatings. The resultant USTC-6@GO@sponge sorbent became blue because of the relatively uniform growth and distribution of USTC-6 inside the sponge. With an increased amount of USTC-6 in USTC-6@GO@sponge, the water contact angle and hydrophobicity of the sorbent gradually increase up to 121°–130°, whereas oil droplets readily permeate this sorbent. This indicates that it satisfactorily inherits the hydrophobic/oleophilic nature of USTC-6, and the incorporation of USTC-6 dramatically changes the properties of GO@sponge (Supplementary Figures S7, S8, S10 and Supplementary

Scheme 2 Illustration of the experimental apparatus for the *in situ* consecutive collection of oil on the surface of water into the recovery vessel. The oil and the water are colored blue and red, respectively, for clear presentation.

Video S1). Because of its low density, USTC-6@GO@sponge kept floating on the liquid surface of the mixture and selectively adsorbed all of the gasoline in several seconds (Figures 2g–i). Even when USTC-6@GO@sponge was forced into the water, it immediately floated back to the surface of water after the release of pressure, and no water uptake was observed during the procedure (Supplementary Figure S13).

It is noteworthy that the oil adsorption of the USTC-6@GO@sponge sorbent can sustain a wide temperature range from − 40 to 125 °C (Supplementary Figure S11), demonstrating that it is suitable for oil spillage and chemical leakage cleanup at extreme temperatures. The adsorption efficiency can be quantified as the weight gain, wt%, which is defined as the weight of adsorbed oil per unit weight of pristine USTC-6@GO@sponge. Various types of oils and organic solvents widely used in our daily life or industry were investigated, including commercial petroleum products, aromatic compounds, hydrocarbon solvents and even soybean oil. USTC-6@GO@sponge exhibited very high adsorption capacities for all of these oils and organics ranging from 1200 to 4300 wt% (Figure 2j). In addition, the sorbent is even able to possess a similar adsorption capacity after being immersed in different pH solutions for 24 h (Supplementary Figure S12). The superior adsorption capacity can be mainly attributed to the microporous nature of USTC-6 and the high and hierarchical porosity of the sorbent. The adsorbed oils can be readily recovered by squeezing USTC-6@GO@sponge, which has good elasticity and mechanical stability based on a synergistic effect from the three components: the sponge offers a macroporous matrix with elasticity; the USTC-6 particles possess microporosity and great hydrophobicity for the selective adsorption of organic compounds over water; and the GO allows USTC-6 to firmly coat the sponge via coordination bonding. Although PCPs have been intensively reported for various applications, especially as sorbents for molecular sorption and separation,[16–19] to the best of our knowledge, this is the first example of a PCP-containing composite material with a superior adsorption capacity for diverse oils/organic solvents.

Given that the adsorption-squeezing operation needs to be repeated countless times in a practical oil spill cleanup, the procedure would be extremely tedious and not energy efficient. Recently, Yu *et al.* have
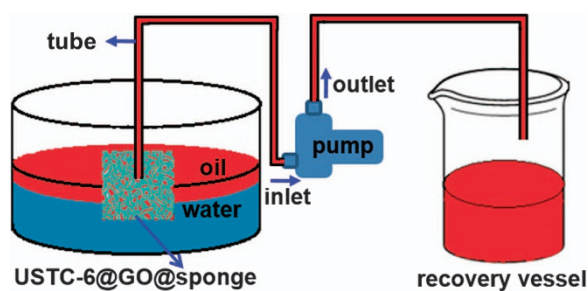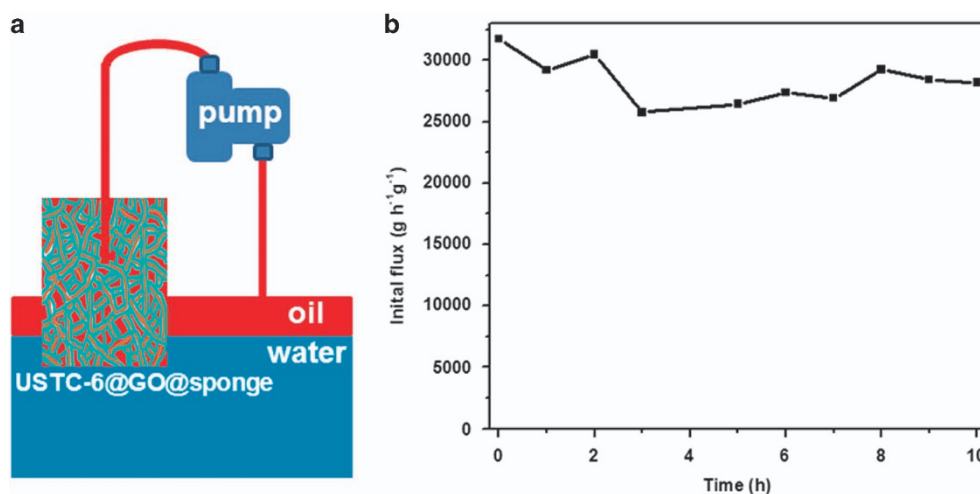
Figure 3 Long-term continuous operation ability was demonstrated by 10 h of continuous separation and recovery of hexane from water without a noticeable decrease in efficiency: (**a**) a circulatory system employed for the demonstration of the consecutive oil collection capabilities of this apparatus and (**b**) a plot of the flux of oil (*n*-hexane) versus time with such a system. The voltage for Mini Electric Motor 360 S is 4.5 V, and the inner diameter of tube is 1.5 mm (outer: 2 mm). The volumes of the oil and water are 30 and 150 ml, respectively, in a 250-ml beaker.
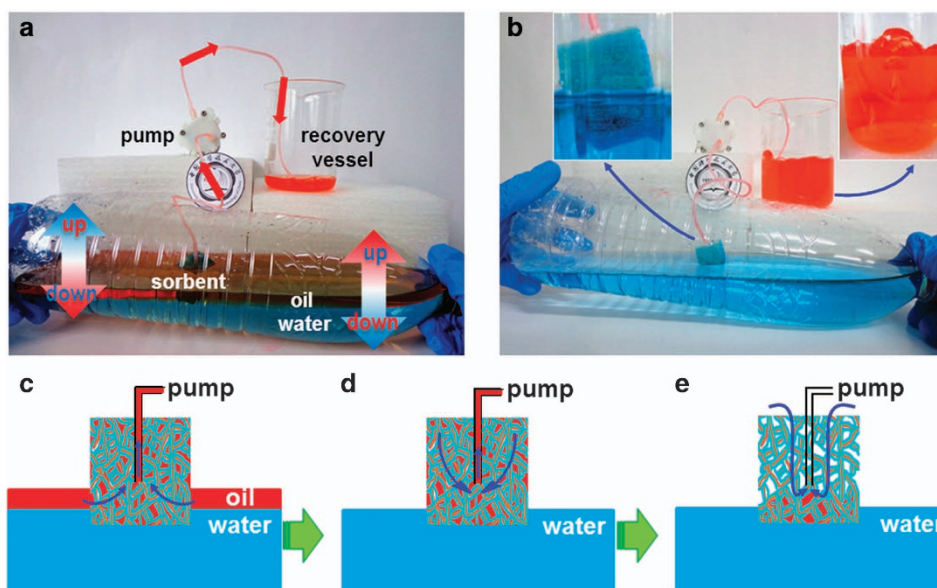
Figure 4 Photographs showing (**a**) the apparatus continuously collecting the floating oil (dyed red) on the surface of water (dyed blue) in motion and (**b**) the status after removing all of the oil on the water surface. Insets in (**b**) show the enlarged sorbent and air bubbles. (**c**–**e**) An illustration of the oil recovery process with the three main stages accompanied by a pressure change in the oil–air and oil–water interfaces; (**c**) the floating oil is being aspirated; (**d**) the adsorbed oil above the tube nozzle is being removed; and (**e**) the air channel formed inside the sorbent, and only air can be aspirated.
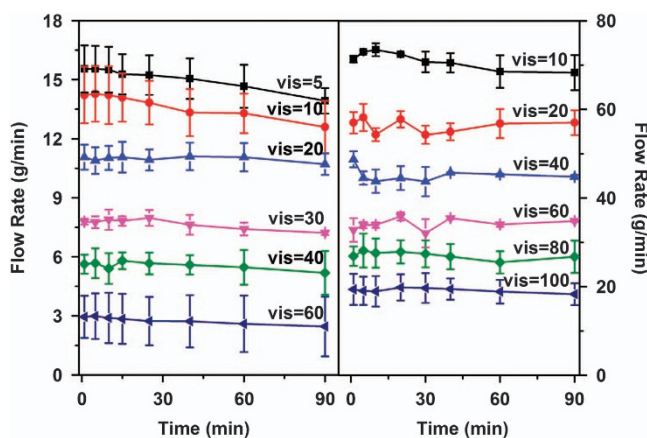

Figure 5 The flow/pumping rate of oils with different viscosities (simplified as 'vis') vs time based on the apparatus assembled with the USTC-6@GO@sponge sorbent, a self-priming pump and tubes: (left) the voltage for Mini Electric Motor 360 S and the inner diameter of the tube are 4 V and 1.5 mm (outer: 2 mm), respectively. (Right) The voltage for the diaphragm pump R385 and the inner diameter of the tube are 12 V and 3.5 mm (outer: 5 mm), respectively.

domonstrated that pumping through porous oil sorbent could realize the continous collection of oil spills *in situ* from water surface, which greatly reduce the materials consumption and simply the oil recovery processes.[7] Therefore, by introducing a pumping force to the USTC--6@GO@sponge sorbent, the oil spill might be selectively and continuouly collected. To domonstrate this assumption, we have prepared a bench-scale apparatus as shown in Scheme 2. Tubes were used to connect the USTC-6@GO@sponge sorbent, the pump and the recovery vessel. Once the pump was powered on, the adsorbed oil rapidly flowed through the tubes to the recovery vessel driven by the suction force, and the remaining oil on the water surface can be consecutively removed through the sorbent until all of the oil is gone (Supplementary Video S2 and Supplementary Figure S14). The whole process is very efficient, which saved not only the sorbent but also labor and operation time.

The oil/water separation and oil recovery model apparatus may find applications extendable to marine oil spillage. The long-term operation ability of the apparatus has been demonstrated by a 10-h successive recovery of hexane from water without a noticeable decrease in efficiency (Figure 3). To further examine its long-term stability and recyclability, the recovery of oil with a viscosity of 30 mPa•s, which is closer to practical demands, was carried out, and the experiment gave well retained efficiency in 8 h (Supplementary Figure S15). In addition, given the harsh conditions in the sea, such as strong winds, powerful waves and extreme weather, the apparatus should be able to withstand those environments.[7] As presented in Figure 4a, to simulate the marine waves, the mixed liquid was manually shaken, and the oil separation/recovery proceeded smoothly with only a slightly longer duration because of the relatively reduced possibility of contact between the oil and the sorbent in motion. After the oil recovery was completed, no water adsorption was observed, but several air bubbles

appeared in the collection vessel (Figure 4b and Supplementary Video S3), indicating that an air channel was formed inside the hierarchically porous sorbent to terminate the liquid suction. The capillary pressures at oil–air and oil–water interfaces inside the sorbent are assumed to be key factors for the suction power regulation, which allow the smooth separation and recovery of oil, whereas no water can be aspirated by this apparatus.[7] At the initial stage, the adsorbed oil inside the sorbent, having been drawn up by the capillary force at the oil–air interface, is aspirated once the pump is switched on. Under the suction force, the pressure at the nozzle of the tube decreases, whereas the capillary pressures at the oil–air and oil–water interfaces increase (Figure 4c). Therefore, the floating oil surrounding the sorbent continually penetrates the sorbent and is pumped into the recovery vessel. When the floating oil is close to depletion, the pressure at the oil–air interface quickly increases to an unsustainable limit for the suction force (Figure 4d). When the oil above the nozzle of the tube is completely removed, air channels above its bottom are formed inside the sorbent, whereas the remaining oil below the tube is left behind. In this case, only air is aspirated and flows along the tubes to the collection vessel, resulting in air bubbles (Figure 4e and Supplementary Video S3). The water permeation to the sorbent is prohibited, and no water uptake is observed during the process.

It is noteworthy that the water contact angle of the USTC-6@GO@sponge sorbent is approximately 128° and that oil removal can be carried out even in water of high salinity ($NaCl > 15\%$), implying a feasibility for practical oil recovery from sea water (NaCl: 3–3.5%). In addition, the recovery of diverse organic solvents (generally with low viscosity) and oils with a viscosity up to 100 mPa•s, surpassing that of common crude oils (approximately 50 mPa•s), was also preliminarily demonstrated to be feasible using the USTC-6@GO@sponge sorbent (Figure 5, left). Although the pumping rate becomes slow when the viscosity becomes very high, this issue can fortunately be improved to a certain degree by using an apparatus with a larger tube diameter, a high-power pump and higher voltage (Figure 5, Supplementary Figures S16 and S17; Supplementary Information, Section 2).

CONCLUSION

In summary, a novel hydrophobic PCP, USTC-6 with a low-energy surface functionalized by -CF$_3$ groups was rationally synthesized. USTC-6 exhibits an exceptional stability toward both acidic and basic solutions (pH 2–10). The *in situ* growth of USTC-6 throughout GO@sponge endows the resultant USTC-6@GO@sponge sorbent with good hydrophobicity/oleophilicity. This hierarchically porous sorbent takes up as much as 1200–4300 wt% of organic pollutants and oils, and it can separate oil/organic solvents from water by adsorption and wringing. Remarkably, a simple model apparatus based on the sorbent leads to the successive recovery of oil spillage from water, and the current system possesses some special advantages: (1) the oil recovery can proceed continuously without human intervention, greatly saving sorbent, labor and operation time compared with the previous 'adsorption-squeezing' process;[7,9–12] (2) the recovery of diverse organic solvents and oils with a viscosity up to 100 mPa•s is approved; (3) the sorbent endures extreme temperatures (−40 to 125 °C) well; (4) the apparatus is workable with marine waves in sea water or even high saline water; and (5) the long-term operation ability of the apparatus was preliminarily demonstrated. This is the first work with a PCP applied to the large-scale separation and recovery oils/organic solvents from water. Given its facile fabrication and continuous operation without a capacity limit, as well as its portability, such a USTC-6@GO@sponge-based apparatus holds great potential in the emergent cleanup of water pollution.

CONFLICT OF INTEREST

The authors declare no conflict of interest.

1 Field, R. W. Surface science: separation by reconfiguration. *Nature* **489**, 41–42 (2012).
2 Adebajo, M. O., Frost, R. L., Kloprogge, J. T., Carmody, O. & Kokot, S. Porous materials for oil spill cleanup: a review of synthesis and absorbing properties. *J. Porous Mater.* **10**, 159–170 (2003).
3 Tuteja, A., Choi, W., Ma, M., Mabry, J. M., Mazzella, S. A., Rutledge, G. C., McKinley, G. H. & Cohen, R. E. Designing superoleophobic surfaces. *Science* **318**, 1618–1622 (2007).
4 Yao, X., Song, Y. & Jiang, L. Applications of bio-inspired special wettable surfaces. *Adv. Mater.* **23**, 719–734 (2011).
5 Gui, X., Wei, J., Wang, K., Cao, A., Zhu, H., Jia, Y., Shu, Q & Wu, D Carbon nanotube sponges. *Adv. Mater.* **22**, 617–621 (2010).
6 Hayase, G., Kanamori, K., Fukuchi, M., Kaji, H. & Nakanishi, K. Facile synthesis of marshmallow-like macroporous gels usable under harsh conditions for the separation of oil and water. *Angew. Chem. Int. Ed.* **52**, 1986–1989 (2013).
7 Ge, J., Ye, Y.-D., Yao, H.-B., Zhu, X., Wang, X., Wu, L., Wang, J.-L., Ding, H Yong, N, He, L.-H. & Yu, S. H. Pumping through porous hydrophobic/oleophilic materials: an alternative technology for oil spill remediation. *Angew. Chem. Int. Ed.* **53**, 3612–3616 (2014).
8 Lei, W., Portehault, D., Liu, D., Qin, S. & Chen, Y. Porous boron nitride nanosheets for effective water cleaning. *Nat. Commun* **4** (), 1–7 (2013).
9 Li, A., Sun, H.-X., Tan, D.-Z., Fan, W.-J., Wen, S.-H., Qing, X.-J., Li, G. X., Li, S. Y. & Deng, W. Q. Superhydrophobic conjugated microporous polymers for separation and adsorption. *Energy Environ. Sci.* **4**, 2062–2065 (2011).
10 Nguyen, D. D., Tai, N.-H., Lee, S.-B. & Kuo, W.-S. Superhydrophobic and super-oleophilic properties of graphene-based sponges fabricated using a facile dip coating method. *Energy Environ. Sci.* **5**, 7908–7912 (2012).
11 Bi, H., Xie, X., Yin, K., Zhou, Y., Wan, S., He, L., Xu, F., Banhart, F., Sun, L. & Ruoff, R. S. Spongy graphene as a highly efficient and recyclable sorbent for oils and organic solvents. *Adv. Funct. Mater.* **22**, 4421–4425 (2012).
12 Liang, H.-W., Guan, Q.-F., Chen, L.-F., Zhu, Z., Zhang, W.-J & Yu, S.-H. Macroscopic-scale template synthesis of robust carbonaceous nanofiber hydrogels and aerogels and their applications. *Angew. Chem. Int. Ed.* **51**, 5101–5105 (2012).
13 Long, J. R. & Yaghi, O. M. The pervasive chemistry of metal-organic frameworks. *Chem. Soc. Rev.* **38**, 1213–1214 (2009).
14 Zhou, H.-C., Long, J. R. & Yaghi, O. M. Introduction to metal-organic frameworks. *Chem. Rev.* **112**, 673–674 (2012).
15 Zhou, H.-C. & Kitagawa, S. Metal-organic frameworks (MOFs). *Chem. Soc. Rev.* **43**, 5415–5418 (2014)) and reference therein.
16 Suh, M. P., Park, H. J., Prasad, T. K. & Lim, D.-W. Hydrogen storage in metal-organic frameworks. *Chem. Rev.* **112**, 782–835 (2012).
17 Li, J.-R., Sculley, J. & Zhou, H.-C. Metal-organic frameworks for separations. *Chem. Rev.* **112**, 869–932 (2012).
18 Tan, Y.-X., He, Y.-P. & Zhang, J. Temperature-/pressure-dependent selective separation of CO$_2$ or benzene in a chiral metal-organic framework material. *ChemSusChem* **5**, 1597–1601 (2012).
19 de Voorde, B. V., Bueken, B., Denayer, J. & De Vos, D. Adsorptive separation on metal-organic frameworks in the liquid phase. *Chem. Soc. Rev.* **43**, 5766–5788 (2014).
20 Seo, J. S., Whang, D., Lee, H., Jun, S. I., Oh, J., Jeon, Y. J. & Kim, K. A homochiral metal–organic porous material for enantioselective separation and catalysis. *Nature* **404**, 982–986 (2000).
21 Farrusseng, D., Aguado, S. & Pinel, C. Metal-organic frameworks: opportunities for catalysis. *Angew. Chem. Int. Ed.* **48**, 7502–7513 (2009).
22 Jiang, H.-L. & Xu, Q. Porous metal-organic frameworks as platforms for functional applications. *Chem. Commun.* **47**, 3351–3370 (2011).
23 Zhang, T. & Lin, W. Metal-organic frameworks for artificial photosynthesis and photocatalysis. *Chem. Soc. Rev.* **43**, 5982–5993 (2014).
24 Gascon, J., Corma, A., Kapteijn, F. & Llabrés i Xamena, F. X. Metal-organic framework catalysis: Quo vadis? *ACS Catal* **4**, 361–378 (2014).
25 Chen, B., Xiang, S. & Qian, G. Metal-organic frameworks with functional pores for recognition of small molecules. *Acc. Chem. Res.* **43**, 1115–1124 (2010).

26 Takashima, Y., Martínez, V., Furukawa, S., Kondo, M., Shimomura, S., Uehara, H., Nakahama, M., Sugimoto, K. & Kitagawa, S. Molecular decoding using luminescence from an entangled porous framework. *Nat. Commun.* **2** (), 1–8 (2011).

27 Kreno, L. E., Leong, K., Farha, O. K., Allendorf, M., Van Duyne, R. P. & Hupp, J. T. Metal-organic framework materials as chemical sensors. *Chem. Rev.* **112**, 1105–1125 (2012).

28 Hu, Z., Deibert, B. J. & Li, J. Luminescent metal-organic frameworks for chemical sensing and explosive detection. *Chem. Soc. Rev.* **43**, 5815–5840 (2014).

29 Wang, Z. & Cohen, S. M. Postsynthetic modification of metal-organic frameworks. *Chem. Soc. Rev.* **38**, 1315–1329 (2009).

30 Kitagawa, H. Metal-organic frameworks: transported into fuel cells. *Nat. Chem* **1**, 689–690 (2009).

31 Burnett, B. J., Barron, P. M., Hu, C. & Choe, W. Stepwise synthesis of metal-organic frameworks: replacement of structural organic linkers. *J. Am. Chem. Soc.* **133**, 9984–9987 (2011).

32 Ramaswamy, P., Wong, N. E. & Shimizu, G. K. H. MOFs as proton conductors – challenges and opportunities. *Chem. Soc. Rev.* **43**, 5913–5932 (2014).

33 Yang, C., Kaipa, U., Mather, Q. Z., Wang, X., Nesterov, V., Venero, A. F. & Omary, M. A. Fluorous metal-organic frameworks with superior adsorption and hydrophobic properties toward oil spill cleanup and hydrocarbon storage. *J. Am. Chem. Soc.* **133**, 18094–18097 (2011).

34 Férey, G., Mellot-Draznieks, C., Serre, C., Millange, F., Dutour, J., Surblé, S. & Margiolaki, I. A chromium terephthalate-based solid with unusually large pore volumes and surface area. *Science* **309**, 2040–2042 (2005).

35 Park, K. S., Ni, Z., Côté, A. P., Choi, J. Y., Huang, R., Uribe-Romo, F. J., Chae, H. K., O'Keeffe, M. & Yaghi, O. M. Exceptional chemical and thermal stability of zeolitic imidazolate frameworks. *Proc. Natl Acad. Sci. USA* **103**, 10186–10191 (2006).

36 Huang, X. C., Lin, Y. Y., Zhang, J. P. & Chen, X. M. Ligand-directed strategy for zeolite-type metal-organic frameworks: zinc(II) imidazolates with unusual zeolitic topologies. *Angew. Chem. Int. Ed.* **45**, 1557–1559 (2006).

37 Cavka, J. H., Jakobsen, S., Olsbye, U., Guillou, N., Lamberti, C., Bordiga, S. & Lillerud, K. P. A new zirconium inorganic building brick forming metal organic frameworks with exceptional stability. *J. Am. Chem. Soc.* **130**, 13850–13851 (2008).

38 Colombo, V., Galli, S., Choi, H. J., Han, G. D., Maspero, A., Palmisano, G., Masciocchi, N. & Long, J. R. High thermal and chemical stability in pyrazolate-bridged metal-organic frameworks with exposed metal sites. *Chem. Sci.* **2**, 1311–1319 (2011).

39 Devic, T. & Serre, C. High valence 3p and transition metal based MOFs. *Chem. Soc. Rev.* **43**, 6097–6115 (2014).

40 Jiang, H.-L., Feng, D., Wang, K., Gu, Z.-Y., Wei, Z., Chen, Y.-P. & Zhou, H.-C. An exceptionally stable, porphyrinic Zr metal-organic framework exhibiting pH-dependent fluorescence. *J. Am. Chem. Soc.* **135**, 13934–13938 (2013).

41 Nguyen, J. G. & Cohen, S. M. Moisture-resistant and superhydrophobic metal-organic frameworks obtained via postsynthetic modification. *J. Am. Chem. Soc.* **132**, 4560–4561 (2010).

42 Aguado, S., Canivet, J. & Farrusseng, D. Engineering structured MOF at nano and macroscales for catalysis and separation. *J. Mater. Chem.* **21**, 7582–7588 (2011).

43 Chen, T.-H., Popov, I., Zenasni, O., Daugulis, O. & Miljanic, O. S. Superhydrophobic perfluorinated metal-organic frameworks. *Chem. Commun.* **49**, 6846–6848 (2013).

44 Padial, N. M., Procopio, E. Q., Moncoro, C., López, E., Oltra, J. E., Colombo, V., Maspero, A., Masciocchi, N., Galli, S., Senkovska, I., Kaskel, S., Barea, E. & Navarro, J. A. R. Highly hydrophobic isoreticular porous metal-organic frameworks for the capture of harmful volatile organic compounds. *Angew. Chem. Int. Ed.* **52**, 8290–8294 (2013).

45 Rao, K. P., Higuchi, M., Sumida, K., Furukawa, S., Duan, J. & Kitagawa, S. Design of superhydrophobic porous coordination polymers through the introduction of external surface corrugation by the use of an aromatic hydrocarbon building unit. *Angew. Chem. Int. Ed.* **53**, 8225–8230 (2014).

46 Wu, T., Shen, L., Luebbers, M., Hu, C., Chen, Q., Ni, Z. & Masel, R.I. Enhancing the stability of metal-organic frameworks in humid air by incorporating water repellent functional groups. *Chem. Commun.* **46**, 6120–6122 (2010).

47 Decoste, J. B., Peterson, G. W., Smith, M. W., Stone, C. A. & Willis, C. R. Enhanced stability of Cu-BTC MOF via perfluorohexane plasma-enhanced chemical vapor deposition. *J. Am. Chem. Soc.* **134**, 1486–1489 (2012).

48 Shibuichi, S., Onda, T., Satoh, N. & Tsujii, K. Super water-repellent surfaces resulting from fractal structure. *J. Phys. Chem.* **100**, 19512–19517 (1996).

49 Nishino, T., Meguro, M., Nakamae, K., Matsushita, M. & Ueda, Y. The lowest surface free energy based on $-CF_3$ alignment. *Langmuir* **15**, 4321–4323 (1999).

50 Ge, J., Yao, H.-B., Hu, W., Yu, X.-F., Yan, Y.-X., Mao, L.-B., Li, H.-H., Li, S-S. & Yu, S.-H. Facile dip coating processed graphene/MnO_2 nanostructured sponges as high performance supercapacitor electrodes. *Nano Energy* **2**, 505–513 (2013).

51 Sheldrick, G. M. *SHELXTL NT, Program for Solution and Refinement of Crystal Structures, Version 5.1* (University of Göttingen, Germany, 1997).

Supplementary Information accompanies the paper on the NPG Asia Materials website (http://www.nature.com/am)